



Deposited via The University of Sheffield.

White Rose Research Online URL for this paper:

<https://eprints.whiterose.ac.uk/id/eprint/174642/>

Version: Published Version

---

**Article:**

Poluri, N. and DeSouza, M.M. (2021) Designing a broadband amplifier without loadpull. IEEE Microwave and Wireless Components Letters, 31 (6). pp. 593-596. ISSN: 1531-1309

<https://doi.org/10.1109/lmwc.2021.3061804>

---

© 2021 IEEE. Personal use of this material is permitted. Permission from IEEE must be obtained for all other users, including reprinting/ republishing this material for advertising or promotional purposes, creating new collective works for resale or redistribution to servers or lists, or reuse of any copyrighted components of this work in other works. Reproduced in accordance with the publisher's self-archiving policy.

**Reuse**

Items deposited in White Rose Research Online are protected by copyright, with all rights reserved unless indicated otherwise. They may be downloaded and/or printed for private study, or other acts as permitted by national copyright laws. The publisher or other rights holders may allow further reproduction and re-use of the full text version. This is indicated by the licence information on the White Rose Research Online record for the item.

**Takedown**

If you consider content in White Rose Research Online to be in breach of UK law, please notify us by emailing [eprints@whiterose.ac.uk](mailto:eprints@whiterose.ac.uk) including the URL of the record and the reason for the withdrawal request.

# Designing a broadband amplifier without Load-Pull

Nagaditya Poluri, *Member, IEEE*, and Maria Merlyne De Souza, Sr., *Member, IEEE*

**Abstract**—The design of a broadband amplifier without using Load-Pull is described. This approach relies on a coarse model of the power amplifier, in which matching networks are represented by rational polynomials and the device by its large-signal model. A simultaneous search of the impedance space and possible matching networks via particle swarm optimization can identify the design solution. The prototype amplifier demonstrates an outstanding gain of 12.8 – 14.9 dB with  $\pm 1$  dB gain flatness, output power greater than 40 dBm, and efficiency between 51-70% over a target frequency range of 2.4-4.6 GHz, the highest frequency range using the CGH40010 to date. The measured two-tone third-order intermodulation (IMD3) is lower than -20 dBc up to an average output power of 38.7 dBm for frequencies less than 4.2 GHz. The impedances obtained by our approach converge within the high-efficiency region identified by the conventional load-pull approach.

**Index Terms**—Broadband Power amplifier, Simplified Real Frequency Technique.

## I. INTRODUCTION

FUTURE wireless communication systems such as 5G require high-efficiency wide bandwidth power amplifiers. A typical amplifier design procedure consists of two steps: 1) Identifying and choosing the impedances, often using load-pull, for high and constant performance (efficiency, output power, ACPR) over the bandwidth. Alternatively, theoretical impedances at the intrinsic plane, calculated based on the current and voltage waveforms, can be transformed to the extrinsic plane [1][2][3]. However, not all such impedances are realizable, because the passive network must have a clockwise trajectory with frequency on the Smith chart to be realisable [4]. 2) Designing a matching network to achieve these impedances with minimal discrepancy. Matching network topologies such as the double stub [2], Chebyshev transformer with a short transmission line [5], filters such as elliptic [6], stepped impedance [7], Ring-Resonator [8], bandpass and lowpass [9] [10] have been shown to achieve high efficiency (>60%) over fractional bandwidths ranging from 40-140 % below 4 GHz at powers of 10-16W. In particular, filter-based matching networks are easier to design, as the theory provides an available framework to synthesize a network for a given frequency band. Similar to filter theory, real frequency techniques (RFT) [11] avoid an a priori choice of a topology of matching network by representing impedances as a rational

function of frequency, although these are not restricted to the filtering response. RFT based approaches have been successfully demonstrated in [12], [13] and [14] for the design of amplifiers with bandwidths greater than 63% at sub-3 GHz frequency at 10 W- 16 W of power levels. An automated design approach is proposed in [15] in which RFT is used to synthesize several matching network topologies that match the optimal impedance iteratively until optimization goals (efficiency, output power etc.,) are met.

On the other hand, instead of a two-step approach, methods that directly relate the performance to the network topology have benefited from a simplification of the above sequential approach. For example, an explicit analytical relationship between a pre-selected load network and the optimal voltage and current waveforms were derived for a Class-E mode in [16]. This allowed the authors to directly predict the optimal efficiency with the corresponding matching network values. However, in their approach, the matching network topology is decided a priori and a closed-form analytical expression for the impedances need to be derived for the chosen matching network; hence, limited by the complexity of the matching network. In [17], we presented a systematic approach for the broadband amplifier design which simultaneously identifies the topology of the matching network at the same time as the impedances for target efficiency and output power. However, in [17], this approach has been demonstrated only in simulations. This paper proves the idea proposed in [17] via a prototype and the approach has been compared with the conventional Load-Pull technique. The measured performance (efficiency, output power) is compared with literature and the measured linearity of the fabricated prototype is presented.

## II. ILLUSTRATION OF THE AMPLIFIER DESIGN APPROACH

The design of a 2.6-4.6 GHz amplifier based on a contiguous mode [18] using a 10 W GaN HEMT from Wolfspeed, CGH40010F is illustrated. The device is biased at drain voltage ( $V_{dsq}$ ) and current ( $I_{dsq}$ ) of 28 V and 150 mA respectively. The design approach [17] relies on two levels of accuracy in the modelling approach as shown in Fig. 1:

1) A coarse model of the amplifier in which the S-parameters of the matching networks are represented in a rational form whereas the device is represented by its large-signal model. In this work, S-parameters are expressed as rational functions of

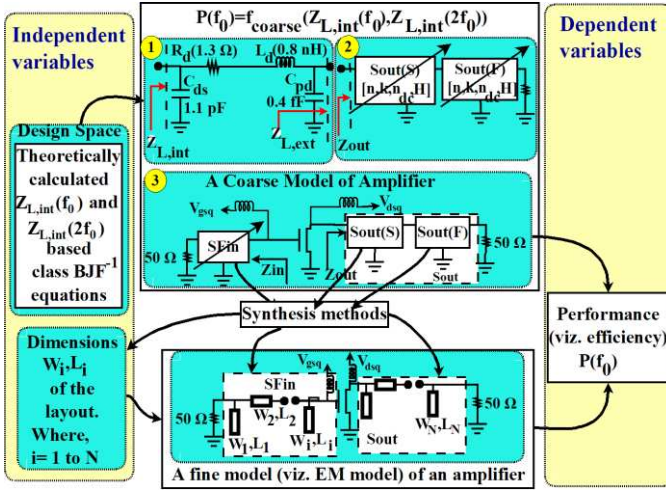


Fig. 1. The coarse and fine models in our design approach.  $f_{coarse}(\cdot)$  is a function which associates each impedance in the design space with the performance of the coarse model. Three steps in the calculation of  $f_{coarse}(\cdot)$  are shown. The drain parasitic used for embedding in step 1 consists of drain source capacitance ( $C_{ds}$ ) in parallel with an RLC network consisting of  $R_d$ ,  $L_d$ , and  $C_{pd}$ . The RLC network models effects from both the package and extrinsic parasitics at the drain terminal.

$\lambda$ , where the frequency is mapped in the  $\lambda$ -domain using Richard's transformation [19]. The S parameters of an ideal lossless passive network in the  $\lambda$ -domain can be completely defined by an array  $[n, n_{dc}, k, H = \{h_n, h_{n-1}, \dots, h_1\}]$ , where  $n$  denotes the number of the elements in the matching network,  $H$  represents a set of real numbers related to the characteristic impedance of elements,  $n_{dc} \in \mathbb{Z}$  denotes the number of DC zeros to be synthesized as short stubs, and  $k$  denotes the number of transmission lines in the matching network [19][20]. The advantage of the coarse model when compared to the black-box model such as Bayesian [21]/Gaussian regression[22] is that this model retains the physical properties of the matching network and the layout of the amplifier can be generated using synthesis algorithms as demonstrated in [19][20].

2) a fine model consists of the conventional EM model of the layout of matching networks as undertaken in Momentum/FEM in ADS along with the large-signal model of the device.

At a frequency  $f_0$ , the association between each set of the fundamental and second harmonic impedances in the design space ( $Z_{L,int}(f_0), Z_{L,int}(2f_0)$ ), with the performance (PAE, output power) of the coarse model of the amplifier ( $P(f_0)$ ), is denoted by a function  $f_{coarse}(Z_{L,int}(f_0), Z_{L,int}(2f_0))$ . In this work,  $f_0$  is an array of frequencies [2.6 GHz, 3.15 GHz, 3.7 GHz, 4.25 GHz, 4.5 GHz]. The calculation of  $f_{coarse}(\cdot)$  at  $f_0$  consists of the following steps:

**Step 1:** The theoretical impedances ( $Z_{L,int}(f_0)$  and  $Z_{L,int}(2f_0)$ ) are translated to the extrinsic plane ( $Z_{L,ext}(f_0)$  and  $Z_{L,ext}(2f_0)$ ) using the approximate drain parasitic network, extracted from the vendor model of the device [23], shown in Fig. 1.

**Step 2:** The output matching network consists of two segments Sout(S) and Sout(F) at the fundamental and second harmonic frequencies respectively. S-parameters (ie.,  $n_{dc}, k, H$ ) of the segments Sout(F), and Sout(S) are optimized to meet the extrinsic impedances ( $Z_{L,ext}(f_0)$  and  $Z_{L,ext}(2f_0)$ ). A lower weight (1/10) is given to the matching at the second harmonic.

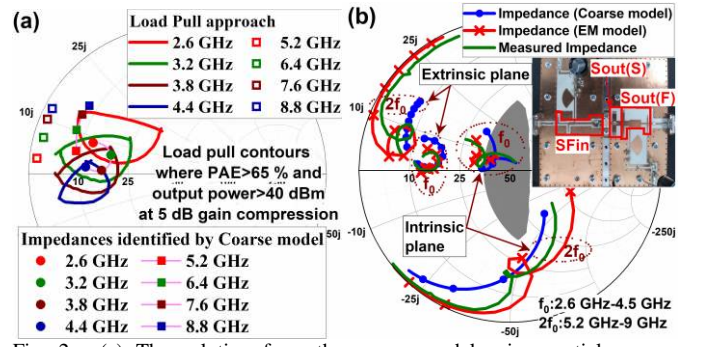


Fig. 2. (a) The solution from the coarse model using particle swarm optimization (PSO). The loadpull contours for efficiency and output power are plotted for comparison. (b) The fundamental and second harmonic load impedances of the coarse model, EM model and the measurement of the output matching network at the intrinsic and extrinsic device planes. The design space used in this work is highlighted in gray. (inset): Photograph of the designed amplifier.

TABLE I  
THE OPTIMAL SIN, SOUT(S) AND SOUT(F) FROM THE ALGORITHM

	n	k	$n_{dc}$	H
Sout(S)	3	2	0	[0.44, -0.23, -3.12, 0]
Sout(F)	6	3	0	[ $10^{-6}$ , -0.90, -1.58, -4.38, -3.19, -2.98, 0]
Sin	7	4	0	[ $-2.0 \times 10^{-06}$ , 1.39, -5.29, -10.26, -5.88, -5.8, 0.15, 0]

**Step 3:** The S-parameters of the input matching network (SFin) are optimized to achieve a flat gain over the bandwidth. Large signal simulations are performed on the coarse model to obtain the power-added-efficiency (PAE) of the amplifier ( $P(f_0)$ ).

The mathematical formulation of  $f_{coarse}(\cdot)$  is presented in detail in [17].  $Z_{L,int}(f_0)$  and  $Z_{L,int}(2f_0)$  are initialized at random from the design space and the optimal  $Z_{L,int}(f_0)$  and  $Z_{L,int}(2f_0)$  that maximize the average  $P(f_0)$  (ie., PAE) over  $f_0$  are obtained using particle swarm optimization (PSO). The number of elements ( $n$ ) of SFin, Sout(S), and Sout(F) are optimized for satisfactory results. For each evaluation of  $f_{coarse}(\cdot)$  during its optimization, several matching networks are implicitly evaluated by steps 2 and 3, resulting in simultaneous optimization of both the impedances and the matching networks. The obtained impedances and matching network solutions are given in Fig. 2 (a) and Table I respectively. Efficiency contours  $> 65\%$  and output power  $> 40\text{dBm}$  over the bandwidth, obtained by recursively performing load-pull at fundamental and harmonics frequencies, in a conventional Load-Pull based approach, are also plotted in Fig. 2 (a) for comparison. The impedances obtained by our approach converge within the region identified by load-pull. The load-pull based approach subsequently requires identification of a matching network topology, whose impedances lie the identified region, which can be synthesized using filtering and SRFT techniques. On the other hand, our method inherently finds both the impedances and the possible synthesizable matching networks simultaneously. Additionally, the source matching network is also obtained in this approach. The solution arrived by this approach depends on the accuracy of the parasitic network, choice of the class of amplifier, and the number of elements of the input/output matching network.

The synthesis algorithms [19][20] are used to generate the matching network topology and dimension from Table I, and the fine model is further optimized using a gradient descent

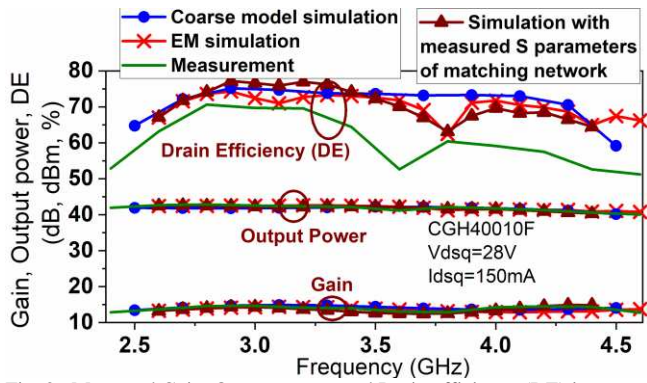


Fig. 3. Measured Gain, Output power, and Drain efficiency (DE) is compared with those predicted from the algorithm, EM simulation and the device simulated with measured S-parameters of input and output matching networks.

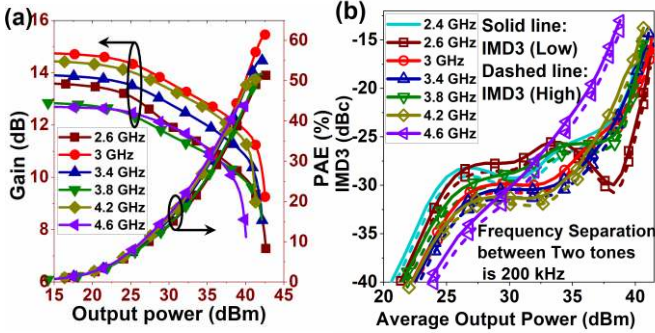


Fig. 4. (a) Measured Gain and efficiency versus input power at frequencies 2.6 GHz, 3 GHz, 3.4 GHz, 3.8 GHz, 4.2 GHz, and 4.6 GHz. (b) Measured third order intermodulation distortion (IMD3) versus the average output power upon application of two-tone signal with the 200 kHz separation between tones with center frequencies 2.4 GHz, 2.6 GHz, 3 GHz, 3.4 GHz, 3.8 GHz, 4.2 GHz, and 4.6 GHz.

algorithm in ADS. The networks synthesized from the parameters in Table I do not have a short stub (since  $n_{dc} = 0$ ) which can be used for biasing. This issue can be overcome by constraining  $n_{dc} > 1$  in  $f_{coarse}(\cdot)$ . The matching networks are fabricated on Rogers 4003C substrate and the photograph of the designed amplifier is shown as inset in Fig. 2 (b).

### III. MEASUREMENT RESULTS

The impedances from the ideal matching network, EM simulation, and measurement are plotted in Fig. 2 (b). The measured impedances closely match with the EM simulated result. It is seen that the fundamental impedances of the coarse model lie in the design space at the intrinsic plane. However, the impedances of the optimized EM model stray out of the design space because, while optimizing the dimensions (length and widths of the transmission lines) of the EM model, the only optimization goal we have set is a minimum difference in performance (Drain Efficiency (DE)) of the coarse and EM model. The DE, output power and Gain of the amplifier with the coarse model, the EM simulation and measurement are plotted in Fig. 3. The gain and output power in both cases remain constant to within 2dB over the bandwidth of 2.4–4.6 GHz and the measured result is accurately predicted by EM simulation. Despite a good match between the efficiency predicted by the optimal particle and EM simulation, measured efficiency shows a 10% reduction for frequencies above 3.2 GHz, with a drop at 3.6GHz. The measured gain and PAE

TABLE II  
COMPARISON OF STATE-OF-THE-ART POWER AMPLIFIERS USING CGH40010F OPERATING BETWEEN FREQUENCIES 2.4 GHz-4.6 GHz

Ref.	Matching Network Synthesis	Freq. of Operation (GHz)	BW <sup>A</sup> (GHz)	Gain (dB)	Pout (dBm)	DE (%)
[7]	Filter	2-3.5	1.5/54.55	13-15.5	40.5-42	64-76
[13]	SRFT	1.7-3	1.3/55.32	--	41.33-42.4	70-79.5
[26]	Apriori	2.4 - 3.9	1.5/47.6	10.7-12.5	39.63-41.4	62-75
[27]	SRFT	1.6-3.5	1.9/74.5	9.4-14.9	40.6-43.1	58-74
[28]	Apriori	3.2-3.7	0.5/14.49	9.9-11.6	40.2-42	70-83
<b>This Proposed Work approach</b>		<b>2.4-4.6</b>	<b>2.2/62.8</b>	<b>12.8-14.9</b>	<b>40-42.8</b>	<b>51-70</b>

<sup>A</sup> BW=Bandwidth; <sup>B</sup> FBW=Fractional BandWidth;

versus output power at frequencies between 2.6 GHz and 4.6 GHz at 0.4 GHz steps are plotted in Fig. 4 (a). The measured peak DE/PAE remains above 50 % (44%) over the entire bandwidth and a peak DE of 70 % is achieved at 2.8 GHz. The average DE/PAE over the bandwidth is 60.3 (52.1) %. To understand the reason for the reduction in measured efficiency, we have simulated the device model with measured S-parameters of the input and output matching networks. The efficiency predicted from this simulation, plotted in Fig. 3, is close to predicted EM simulations, indicating that the mismatch between impedance from measurement and EM simulation has minimal impact on the degradation of efficiency. Therefore, this indicates that the accuracy of the vendor model is critical for the prediction of efficiency, a notoriously difficult parameter to predict. In this regard, approaches based on measured load-pull data, such as those adopted in [24][25], have an advantage.

The third-order intermodulation distortion (IMD3) for a two-tone signal with 200 kHz of tone spacing is plotted in Fig. 4 (b). IMD3 is below -20 dBc up to an average output power of 38.7 dBm at 4.2 GHz, demonstrating good linearity. However, the linearity degrades at this power level beyond 4.2 GHz because the output power of the amplifier saturates earlier, as can be seen in Fig. 4 (a), due to an increase in the real part of the load impedance at the fundamental frequency as seen in Fig. 2 (c). The measured amplifier is compared in Table II with state-of-the-art amplifiers using CGH40010F operating over the frequency range 2.4 GHz- 4.6 GHz, revealing a bandwidth higher than those reported and comparable to [27]. Despite operating at the highest reported frequency for this device, the efficiency is comparable with other PAs at an output power and gain that are excellent by comparison.

### IV. CONCLUSION

We illustrate the design of an amplifier using an approach which considerably simplifies the methodology for broadband amplifiers. Optimization of the coarse model leads to the identification of the optimal impedances that result in high performance (efficiency, output power, etc.,) and the corresponding matching network topology to achieve them. This approach only requires the frequency of operation, device parasitics at the drain, the number of elements in the matching networks and the impedance space of the class of operation as input. Unlike the case of Load-Pull, the device is presented only with impedances realizable by a passive network and the source

matching network is identified simultaneously.

## REFERENCES

- [1] S. C. Cripps, "RF Power Amplifiers for Wireless Communications," 2nd ed., Boston, MA: Artech, 2006.
- [2] K. Mimis, K. A. Morris, S. Bensmida, and J. P. McGeehan, "Multichannel and wideband power amplifier design methodology for 4G communication systems based on hybrid class-J operation," *IEEE Trans. Microw. Theory Tech.*, vol. 60, no. 8, pp. 2562–2570, 2012.
- [3] Q. Li, S. He, W. Shi, Z. Dai, and T. Qi, "Extend the Class-B to Class-J Continuum Mode by Adding Arbitrary Harmonic Voltage Elements," *IEEE Microw. Wirel. Components Lett.*, vol. 26, no. 7, pp. 522–524, 2016.
- [4] S. Saxena, K. Rawat, and P. Roblin, "Continuous Class-B/J Power Amplifier Using Nonlinear Embedding Technique," *IEEE Trans. Circuits Syst. II Express Briefs*, vol. 1, no. 1, pp. 1–1, 2016.
- [5] J. J. Moreno Rubio, V. Camarchia, R. Quaglia, E. F. Angarita Malaver, and M. Pirola, "A 0.6–3.8 GHz GaN Power Amplifier Designed Through a Simple Strategy," *IEEE Microw. Wirel. Components Lett.*, vol. 26, no. 6, pp. 446–448, Jun. 2016.
- [6] M. Yang, J. Xia, Y. Guo, S. Member, A. Zhu, and S. Member, "Highly Efficient Broadband Continuous Inverse Class-F Power Amplifier Design Using Modified Elliptic Low-Pass Filtering Matching Network," *IEEE Trans. Microw. Theory Tech.*, vol. 64, no. 5, pp. 1515–1525, 2016.
- [7] J. Xia, X. W. Zhu, and L. Zhang, "A linearized 2-3.5 GHz highly efficient harmonic-tuned power amplifier exploiting stepped-impedance filtering matching network," *IEEE Microw. Wirel. Components Lett.*, vol. 24, no. 9, pp. 602–604, 2014.
- [8] J. Wang, S. He, F. You, W. Shi, J. Peng, and C. Li, "Codesign of High-Efficiency Power Amplifier and Ring-Resonator Filter Based on a Series of Continuous Modes and Even-Odd-Mode Analysis," *IEEE Trans. Microw. Theory Tech.*, vol. 66, no. 6, pp. 2867–2878, 2018.
- [9] X. Meng, C. Yu, Y. Liu, and Y. Wu, "Design Approach for Implementation of Class-J Broadband Power Amplifiers Using Synthesized Band-Pass and Low-Pass Matching Topology," *IEEE Trans. Microw. Theory Tech.*, pp. 1–13, 2017.
- [10] Q. Cai, W. Che, G. Shen, and Q. Xue, "Wideband High-Efficiency Power Amplifier Using D/CRLH Bandpass Filtering Matching Topology," *IEEE Trans. Microw. Theory Tech.*, vol. 67, no. 6, pp. 2393–2405, 2019.
- [11] H. J. Carlin, "A New Approach to Gain-Bandwidth Problems," *IEEE Trans. Circuits Syst.*, vol. CAS-24, no. 4, pp. 170–175, 1977.
- [12] Y. Sun and X. Zhu, "Broadband Continuous Class F-1 Amplifier With Modified Harmonic-Controlled Network for Advanced Long Term Evolution Application," *IEEE Microw. Wirel. Components Lett.*, vol. 25, no. 4, pp. 250–252, Apr. 2015.
- [13] L. Ma, J. Zhou, and W. Huang, "A Broadband Highly Efficient Harmonic-Tuned Power Amplifier Exploiting Compact Matching Network," *IEEE Microw. Wirel. Components Lett.*, vol. 25, no. 11, pp. 718–720, 2015.
- [14] J. Chen and S. He, "Broadband high-efficiency power amplifiers design based on hybrid continuous modes utilizing the optimal impedances at package plane," in *2015 IEEE MTT-S International Microwave Symposium, IMS 2015*, 2015, no. 3 0, pp. 2–5.
- [15] L. Kouhalvandi, O. Ceylan, and H. B. Yagci, "Power Amplifier Design Optimization with Simultaneous Cooperation of EDA Tool and Numeric Analyzer," *Mediterr. Microw. Symp.*, vol. 2018-October, pp. 202–205, 2019.
- [16] A. Grebennikov, "High-Efficiency Class-E Power Amplifier with Shunt Capacitance and Shunt Filter," *IEEE Trans. Circuits Syst. I Regul. Pap.*, vol. 63, no. 1, pp. 12–22, 2016.
- [17] N. Poluri and M. M. De Souza, "A methodology to design broadband matching networks for continuum mode PAs," in *Asia-Pacific Microwave Conference Proceedings, APMC*, 2019, vol. 2019-December, pp. 1637–1639.
- [18] N. Poluri and M. M. De Souza, "High-Efficiency Modes Contiguous With Class B/J and Continuous Class F<sup>1</sup> Amplifiers," *IEEE Microw. Wirel. Components Lett.*, vol. 29, no. 2, pp. 137–139, Feb. 2019.
- [19] Z. Dai, S. He, F. You, J. Peng, P. Chen, and L. Dong, "A new distributed parameter broadband matching method for power amplifier via real frequency technique," *IEEE Trans. Microw. Theory Tech.*, vol. 63, no. 2, pp. 449–458, 2015.
- [20] A. Grebennikov, N. Kumar, and B. S. Yarman, *Broadband RF and Microwave Amplifiers*. Cambridge: Cambridge University Press, 2016.
- [21] P. Chen, B. M. Merrick, and T. J. Brazil, "Bayesian Optimization for Broadband High-Efficiency Power Amplifier Designs," *IEEE Trans. Microw. Theory Tech.*, vol. 63, no. 12, pp. 4263–4272, 2015.
- [22] P. Chen and T. J. Brazil, "Gaussian processes regression for optimizing harmonic impedance trajectories in continuous class-F power amplifier design," *2015 IEEE MTT-S Int. Microw. Symp. IMS 2015*, no. 3, pp. 1–3, 2015.
- [23] N. Poluri, "Contributing to Second Harmonic Manipulated Continuum Mode Power Amplifiers and On-Chip Flux Concentrators," Department of Electrical and Electronics Engineering, The University of Sheffield, 2020.
- [24] P. Wright, J. Lees, J. Benedikt, P. J. Tasker, and S. C. Cripps, "A methodology for realizing high efficiency class-J in a Linear and Broadband PA," *IEEE Trans. Microw. Theory Tech.*, vol. 57, no. 12, pp. 3196–3204, 2009.
- [25] T. Sharma *et al.*, "High-Efficiency Input and Output Harmonically Engineered Power Amplifiers," *IEEE Trans. Microw. Theory Tech.*, vol. 66, no. 2, pp. 1002–1014, 2018.
- [26] W. Shi, S. He, and Q. Li, "A Series of Inverse Continuous Modes for Designing Broadband Power Amplifiers," *IEEE Microw. Wirel. Components Lett.*, vol. 26, no. 7, pp. 525–527, 2016.
- [27] Z. Dai, S. He, J. Peng, C. Huang, W. Shi, and J. Pang, "A Semianalytical Matching Approach for Power Amplifier With Extended Chebyshev Function and Real Frequency Technique," *IEEE Trans. Microw. Theory Tech.*, vol. 65, no. 10, pp. 3892–3902, 2017.
- [28] Q. Li, S. He, and Z. Dai, "Design of Broadband High-Efficiency Power Amplifiers Based on the Hybrid Continuous Inverse Mode," *IEEE Microw. Wirel. Components Lett.*, vol. 26, no. 1, pp. 4–6, 2016.